CONTROL OF VERTICAL SPINDLE SURFACE GRINDING FROM A MULTI-AXIS NUMERICALLY CONTROLLED MACHINE

Authors: Sheikh Abdullah[1], Syed Irtiza Ali Shah[1], Malik Muhammad Awais[1], Aman Sarwar[1]

[1]Department of Mechanical & Aerospace Engineering Air University Islamabad, Pakistan,
engrshabdullah@gmail.com (Sheikh Abdullah), irtiza@mail.au.edu.pk (Syed Irtiza Ali Shah),
malik.awais19@gmail.com (Malik Muhammad Awais), 170982@students.au.edu.pk (Aman Sarwar)

Received: 22-April-2022 / Revised: 24-June-2022 / Accepted: 06-July-2022
Karachi Institute of Economics and Technology || Technology Forces Journal, Volume 4, Issue 1, 2022

ABSTRACT

Due to the increasing need for components comprised of hard and brittle materials such as glasses, steel alloys, and sophisticated ceramics, standard grinding and polishing techniques are no longer able to meet the expectations of today's precision manufacturing community. Grinding machines' functional capabilities, control systems, and peripheral process monitoring equipment have all improved during the last 20 years. Process enhancement technologies such as touch detection, wheel balancing, and in-process gauging may be incorporated into higher-end grinding machines based on specific customer requirements; however, due to the differing features and functionality of equipment from different suppliers, this requires significant customization work by the manufacturer. Moreover, the execution of long-proposed optimization strategies such as adaptive and intelligent control has not progressed significantly beyond specific research programs tied to a specific machine and controller, frequently using non-industrial equipment for key process data monitoring.However, it is vital and absolutely necessary to carry out such activities using a scientific approach, i.e., the process should be quantitatively controlled and optimized rather than done by trial and error. There is also a need to produce innovative and modern control system for controlled vertical spindle surface grinding multi-axis Computer Numerical Control (CNC) machine.Theoretical modelling and instrumentation for controlled vertical spindle surface grinding multi-axis Computer Numerical Control (CNC) machine are provided and addressed in depth in this study. During the grinding process, a method in which controlling of surface parallelism by changing the depth of cut is done, is applied. The achievable single pass tolerances in vertical spindle surface grinding are frequently restricted by machine compliance and also, the grinding wheel. The approach presented here involves precisely altering the depth of cut during grinding to maximize dimensional precision without the need for additional spark out passes. In this stage, the projected deflection from the simulated compliance and the measured vertical force are utilized to perform the correction. Two distinct methodologies are compared to determine the system's compliance. A controller of multi-axis commercial Computer Numerical Control (CNC) is altered to process the measurement of dynamometer in real-time, calculate controlling commands, and actuate servo loops. Because the system's deflection fluctuates with force of grinding, using depth of cut manipulation, a tracking controller tracks the expected deflection of the wheel, cancelling out part form defects. The results from experiments are shown for a variety of process settings, demonstrating the efficiency in terms of ground part parallelism, of the compensation system. It also resulted in significant improvement in quality of surface grinding.

Keywords: Deflection, Grinding, Depth of cut.

1. INTRODUCTION

Grinding machines are a category of machine tool that performs specific finishing operations on machined components to create a high-quality surface finish and a certain profile. Grinding is the final process done on a component, and it could be done manually for individual components or automatically for manufacturing batches of (similar) components. Conventional hand operated machines needed the operator to rotate control handwheels to move the axes and set numerous switches and limitations to manage mechanically automated features such as axis incremental and reversal infeed or down feed. Their efficiency as well as productivity are virtually entirely determined by the operator's ability and expertise, who will select appropriate increments and speeds based on dimensions and materials, as well as check grinding wheel condition and component quality. Once started, these machines can run semi-autonomously, with the operator changing parts and repeating the cycle as needed. During the 1980s, more sophisticated and complex grinding machines using Computer Numerical Control (CNC) were widely introduced; these allowed full electronic control of axis movements via servo drives, control of machine safety, interfacing to other electronic equipment, and, most importantly, the ability to generate and run complex part-programs that defined the machining operation [1]. Numerical control is a sort of programmable automation in which the process is controlled by numbers, letters, and symbols. Computer Numerical Control (CNC) machining is a manufacturing process that involves the use of computers to control machine tools such as grinders, mills, and lathes.

The most prevalent type of grinding process is surface grinding. It is a common sight in heavy industry, where various metal and nonmetal objects must be refined and smoothed as part of the finishing process.

A surface grinder is made up of a table that holds the abrasive wheel above it. A chuck is a device that holds the item being worked on, known as a workpiece, in place. Surface grinders are classified into three types: vertical spindle, horizontal spindle, single disc grinders, and double disc grinders.

Horizontal spindle grinders: They are ideal for high-precision work on slanted or tapered surfaces, as well as slots or sunken surfaces. They are also known as peripheral grinders.

Single-disc and double-disc grinders: They are available in spindle configurations of both vertical and horizontal directions. These grinders have a greater contact's surface area among the grinding surface and the workpiece and may grind both sides simultaneously. Disc grinders can accept rotors, plates, spacers, gears, and washers.

Vertical-spindle grinders: These grinders also known as wheel-face grinders, and are commonly used for rapid material removal. The face of grinding wheel is lowered onto the workpiece under it. These grinders are best suited for spacers, stops, stators, gears, inner plates, gears and inner rings, as well as wafers and rotors.

The goal of the work presented here is to intelligently control a vertical spindle surface grinding from a multi axis Computer Numerical Control machine.

2. LITERATURE REVIEW

2.1 Prediction T-S Fuzzy Control Method for Prediction of Workpiece' Rotation Speed on grinding machine of Camshaft

Through the studies on non-circular grinding, the manufacturing industry has made a huge breakthrough. This non-circular grinding model is mostly applied on camshaft by China's automobile industry. Through this research we analyze a grinding mathematical model. This mathematical model will help us determine the workpiece's reduction ratio in non-circular section. It can also help us determine the maximum speed of feeding, jerk along with the acceleration of grinding wheel. Through the analysis of feed displacement and acceleration curves of grinding wheel, a linear approximation fuzzy control model of cam rotation was established. Consequently, a rule parameter of fuzzy table was designed, which helped to predict and optimize the cam rotation speed.

Fig. 1 shows the mathematical model of camshaft CNC grinding. The cam's rotation, along C axis, of camshaft grinding machine and grinding wheel's feeding on X axis during the rotation of grinding wheel are controlled by the commands given through CNC.

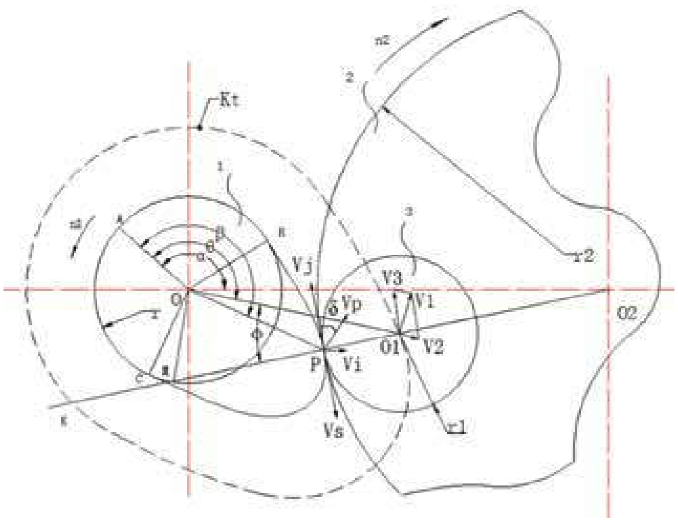

Figure 1: Mathematical model representing CNC camshaft grinding [21].

Here O represents the center of cam base circle's center, O_1 represents the roller measuring head's center. Similarly, O_2 represents the center of grinding wheel.

Here,

Angular velocity at point P =

Angular velocity when the cam rotates to base circle =w_0

Radius of cam base circle is OA = r

Radius of roller measuring head is $PO_1 = r_1$

Radius of grinding wheel is $O_2P = r_2$

Angle of roller measuring head ÐAOO1 = θ

Angle of cam ÐAOO2=$\alpha(\theta)$

Angle between cam and grinding wheel tangent P is DAOP = $\beta(\theta)$.

Similarly, ÐOO1M = φ.

$$X(\theta) = OO_2 - r_2 - r \tag{1}$$

where

$$OO_2 = \sqrt{OO_1^2 + O_1O_2^2 + 2OO_1 \times \cos(\varphi)}$$

Here X(θ) represents feed displacement of grinding wheel.

$O_1O_2 = r_2 - r_1$

$OO_1 = r_2 + H(\theta) + r_1$

Lift value of cam is represented by $H(\theta)$.

$$\varphi = \text{arctg}\frac{OM}{OO_1} = arctg\frac{\frac{dH(\theta)}{d\theta}}{OO_1}$$

$$\alpha(\theta) = \theta - \angle O_2OO_1 = \theta - \arcsin(\frac{\sin(\pi-\varphi)\times O_1O_2}{OO_2}) \tag{2}$$

Similarly when the cam rotates to a (q) the cut-in depth ap is given as

$$a_{ep} = a_p \times \frac{v_j}{v_s} = \frac{Qw'}{v_s} \tag{3}$$

Here linear velocity is being represented by v_s.

On the basis of above equations we proceed further as

$$\omega(\theta) = \frac{\omega_0 \times r}{\sqrt{(\frac{d\rho(\theta)}{d\beta(\theta)})^2 + \rho(\theta)^2 \frac{d\beta(\theta)}{d\alpha(\theta)}}} \tag{4}$$

$$F(\theta) = 360 \times n(\theta) = \frac{10800 \times \omega(\theta)}{\pi} \tag{5}$$

$$where\ v_0 = \omega_0 r \quad , \quad \omega(\theta) = \frac{d\alpha(\theta)}{dt}$$

$$v_s = \omega(\theta)\sqrt{\frac{d\rho(\theta)}{d\beta(\theta)} + \rho(\theta)^2\frac{d\beta(\theta)}{d\alpha(\theta)}}$$

$$\beta(\theta) = \theta + \angle O_2OP = \theta + \arcsin(\frac{\sin(\varphi) \times PO_1}{OP})$$

$$OP = \rho(\theta) = \sqrt{OO_1^2 + PO_1^2 + 2 \times OO_1 \times PO_1 \times \cos(\varphi)}$$

F(θ) and a (θ) they can fit into Eq. (2) and (5) respectively.

The second, third and fourth derivative of the pairs obtained in Eq. (1) are

$$v(\theta) = \frac{d(X(\theta))}{d\theta} \tag{6}$$

$$a(\theta) = \frac{d(v(\theta))}{d\theta} \tag{7}$$

$$j(\theta) = \frac{d(a(\theta))}{d\theta} \tag{8}$$

Here $v(\theta)$, $j(\theta)$, and $a(\theta)$ represent the feeding speed, the jerk, and the acceleration of the grinding wheel, respectively.

Simulations representing connection of Eq. (1), (5), (6), and (7) with Eq. (2) are shown in the graphs below

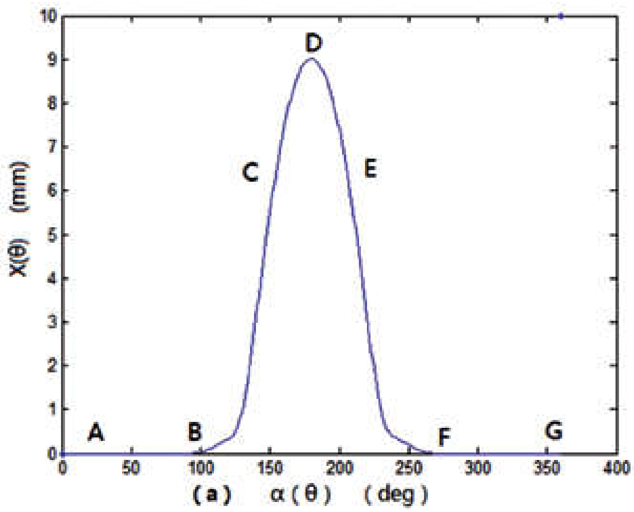

Figure 2(a): Grinding wheel' feed displacement X(θ) curve [21].

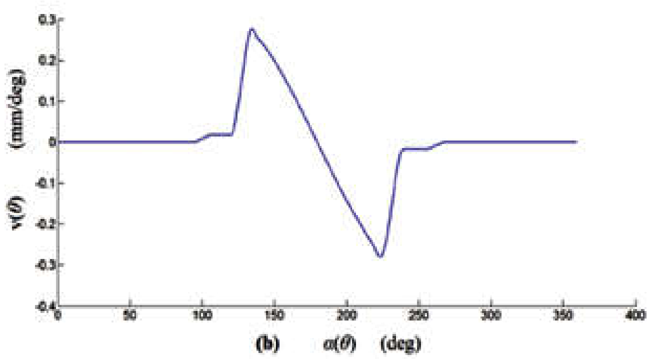

Figure 2(b): Grinding wheel's Feeding speed v(θ) curve [21].

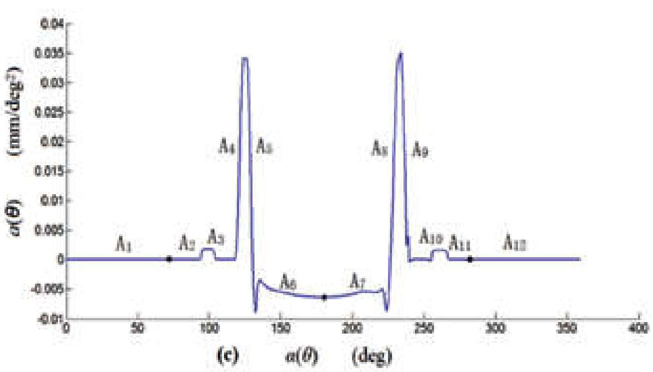

Figure 2(c): Horizontal feeding acceleration a(θ) curve of the grinding wheel [21].

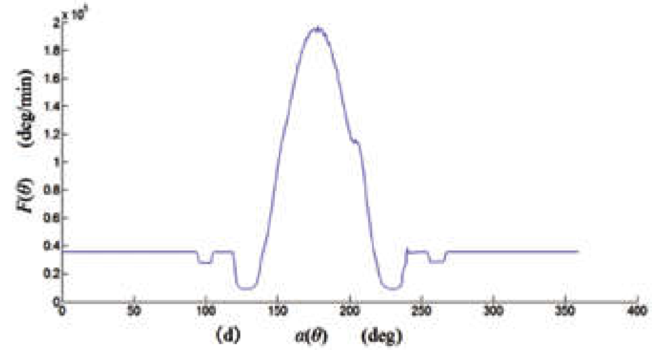

Figure 2(d): Cam's Rotation speed curve [21].

Control method for S shaped acceleration and deceleration is being implemented to counteract the effects of grinding wheel acceleration. For this purpose, the limiting parameters are

$$\begin{cases} v(\theta_i) \leq v_{max} \\ a(\theta_i) \leq a_{max} \\ j(\theta_i) \leq j_{max} \\ k = \frac{\omega_{max}}{1.2\omega_0} \end{cases} \tag{9}$$

$v(\theta i)$, $a(\theta i)$, and $j(\theta i)$ represent the ith interpolation period of feeding speed, acceleration and jerk respectively. Similarly, v_{max}, a_{max}, and j_{max} represent the maximum of feeding speed, acceleration and jerk respectively. Using the displacement curve of feed segmentation of grinding wheel is carried out, which helps to decompose the system into 5 modes of deceleration and acceleration.

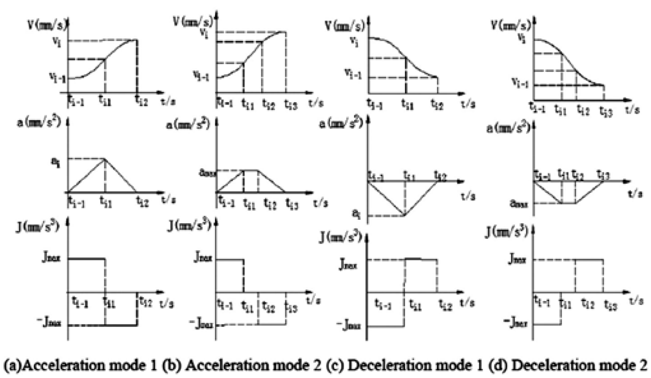

Figure 3: Modes of S-shaped acceleration and deceleration [21].

Here Accleration Mode 1:

$$\begin{cases} s_i(t_{i1}) = v_{i-1}t_{i1} + \frac{1}{6}j_{max}t_{i1}^3 \\ v_{i1} = v_{i-1} + \frac{1}{2}j_{max}t_{i1}^2 \\ t_{i1} = t_{i2} = \frac{T_{si}}{2} \\ s_{i2}(t) = v_{i1}t_{i2} + \frac{1}{2}a_i t_{i2}^2 - \frac{1}{6}j_{max}t_{i2}^3 \\ a_i = \frac{1}{2}j_{max}T_{si} \\ v_{i2} = v_{i1} + a_i t_{i2} - \frac{1}{2}j_{max}t_{i2} = v_{i-1} + \frac{1}{4}j_{max}T_{si}^2 \\ \Delta x_i = s_{i1}(t) + s_{i2}(t) = v_{i-1}T_{si} + \frac{1}{8}j_{max}T_{si}^3 \end{cases} \quad (10)$$

Here s_{i1}(t), s_{i2}(t) are feed displacement in t_{i1} and t_{i2} respectively.

Here s_{i1}(t), *ai*, v_{i1} are the feed displacement, accelerated speed and speed in t_{i1} respectively. Similarly, s_{i2}(t), a_i, v_{i2} are the feed displacement, accelerated speed and speed in ti1 respectively. Interpolation period is represented by T_{si}. Δx_i represents the feed displacement in one interpolation period.

T_{si} is derived with the help of Eq. 10.

Mode 2 of Acceleration:

$$\begin{cases} s_i(t_{i1}) = v_{i-1}t_{i1} + \frac{1}{6}j_{max}t_{i1}^3 \\ v_{i1} = v_{i-1} + \frac{1}{2}j_{max}t_{i1}^2 \\ t_{i1} = t_{i3} = \frac{a_{max}}{j_{max}} \\ v_{i2} = v_{i1} + a_{max}t_{i2} \\ s_{i2}(t_{i2}) = v_{i2}t_{i2} + \frac{1}{2}a_{max}t_{i2}^2 \\ s_{i3}(t_{i3}) = v_{i2}t_{i3} + \frac{1}{2}a_{imax}t_{i3}^2 - \frac{1}{6}j_{max}t_{i3}^3 \\ v_{i3} = v_{i-1} + a_{max}t_{i3} \\ \Delta x_i = s_{i1}(t) + s_{i2}(t) + s_{i3}(t) \\ a_{max}t_{i2}^2 + (j_{max}t_{i1}^2 + 2a_{max}t_{i1} + 2v_{i-1})t_{i2} + \\ 4v_{i-1}t_{i1} + j_{max}t_{i1}^3 + a_{max}t_{i1}^2 - 2\Delta x_i = 0 \\ T_{si} = t_{i1} + t_{i2} + t_{i3} = 2t_{i1} + t_{i2} \end{cases} \quad (11)$$

Uniform acceleration stage's time is represented by t_{i2}. s_{i3}(t) and v_{i3} are feed displacement and speed at t_{i3}.

Eq. (11) can be used to calculate T_{si}.

Similarly,

$$T_w = T_{si} \quad (12)$$

From rotating lift of cam *Tw* and period of interpolation of reciprocating base circle of cam *T₀* the rotation speed Ғ'''' (θ) is calculated as:

$$F''''(\theta) = \frac{T_0}{T_W} \times 36000 = \frac{\frac{1}{600}}{T_W} \times 36000 = \frac{60}{T_W} \quad (13)$$

With this all the acceleration modes are simplified into two acceleration modes.

The feeding acceleration curve and the lift are determined with the help of linear model for the prediction of the rotation of cam.

Once this mathematical model is established a fuzzy control is developed.

The membership function is selected to be a triangle function. The cam's rotation speed curve is modelled and optimized.

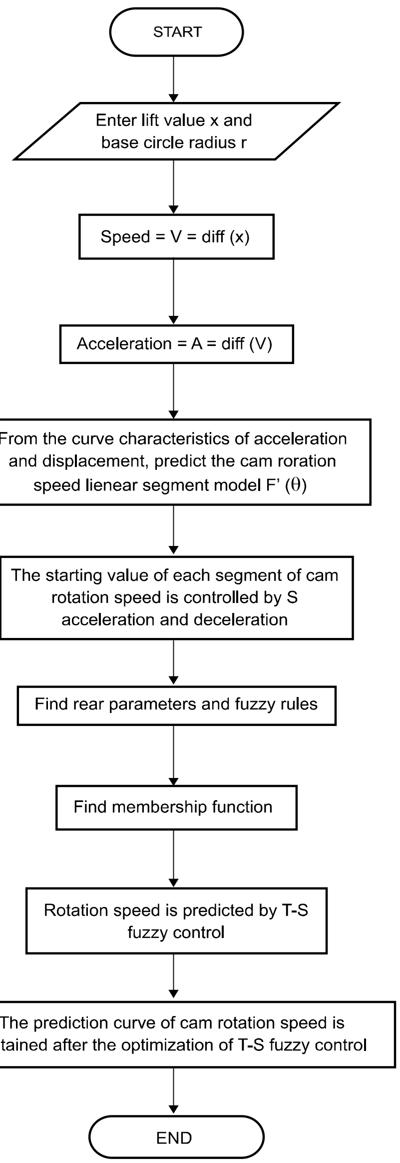

Figure 4: Algorithm representing the process of prediction of rotation speed of cam.

2.2 Grinding's Intelligent Control System

A very intelligent control system for spindle surface grinding machine is proposed here. A schematic of such a control system, which is very intelligent, is shown in Fig. 5.

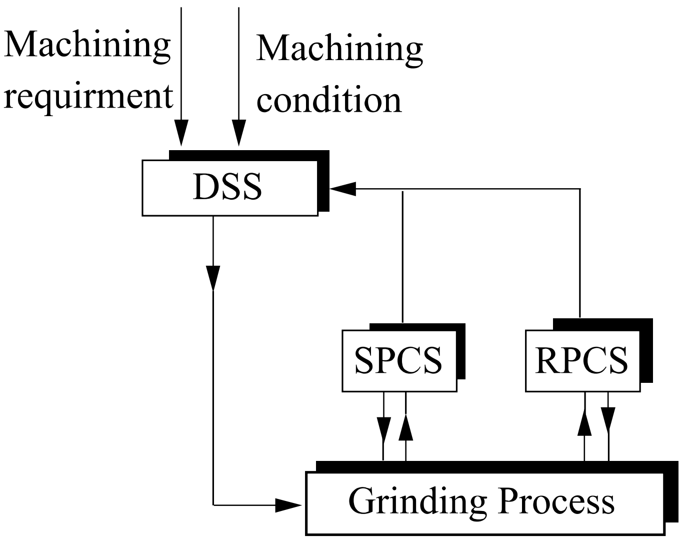

Figure 5: Intelligent control systems schematic diagram [4].

In this process the user enters all the data including workpiece material, dimensional accuracy, machining conditions, spindle type, dimensional accuracy, surface roughness, etc. into DSS.

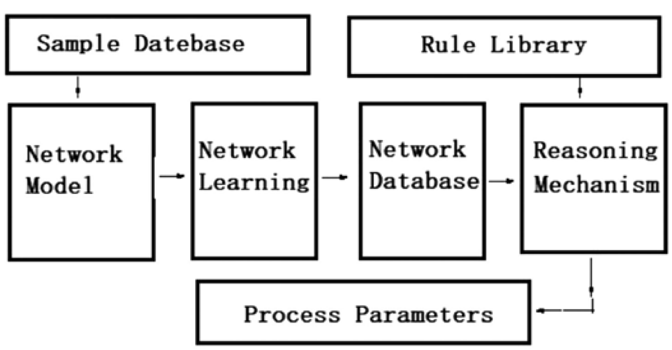

Figure 6: Grinding process parameter DSS construction [4].

A Decision Support System (DSS) is an intelligent system that selects optimal grinding parameters from its expert's library depending on the data provided.

One of the most crucial features of a workpiece is its size. Before the spark-out stage, we construct a size prediction control system (SPCS) to regulate the deformation and size accuracy of workpieces. As shown in Fig. 7, the size prediction control system (SPCS) is made up of three subsystems: deformation control, size prediction, and fuzzy control. In the deformation control subsystem, the optimal adaptive control approach is employed, whereas in the size prediction subsystem, the Elman network with memory is used. First, the grinding parameter decision support system (DSS) determines the best V_f and u for the grinding operation and applies them. Second, the size prediction subsystem is subjected to t (n-1), t'(n-1), t"(n-1), u(n-1) and V_f(n-1). Then t_p(n) can be calculated and fed into subsystem of fuzzy control. The error e and the error change rate e_c can then be calculated using the formulas below:

$$t'_{(n-1)} = t_{(n)} - t_{(n-1)} \quad \text{---(16)}$$
$$t''_{(n-1)} = t_{(n)} - 2t_{(n-1)} + t_{(n-2)} \qquad (14)$$

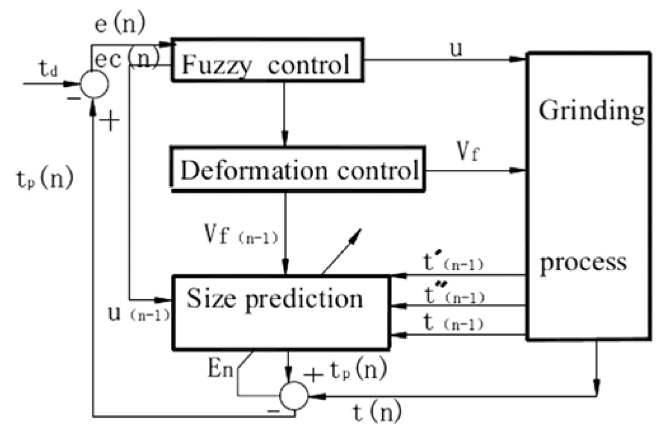

Figure 7: Schematic Diagram of Size Prediction Control System (SPCS) [4].

In the step of spark-out, control of roughness is mostly implemented.

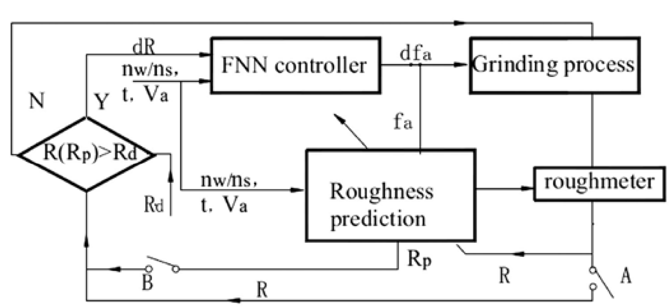

Figure 8: Schematic Diagram of Roughness Prediction Control System (RCPS) [4].

The controller is comprised of a fuzzy neural network (FNN), a prediction subsystem of prediction of surface roughness, and a measurer of roughness. The surface roughness prediction subsystem is a fuzzy neural network-based intelligent system. The amount of workpiece removed is equal to t, the amplitude signal of grinding vibrate is Va, the feed of table is fa, the revolution of workpiece is nw, the revolution of grinding wheel is ns, the roughness that is measured is R, the subsystem for output's prediction of roughness is Rp, the roughness that is desired is Rd, and the change in roughness is dR in Fig. 8. We start by turning on A and turning off B. The rough meter measures the surface roughness of the workpiece and compares it to the desired roughness. The above data is fed into the subsystem for prediction of roughness as the training data of neutral network of fuzzy. As the amount of train data increases, so does the prediction subsystem's accuracy. Switch B is turned on and switch A is turned off when the prediction accuracy meets the criterion. The prediction subsystem of roughness is activated. If roughness does not meet standards, the FNN controller restarts the grinding process. The above-mentioned procedure cycle is repeated again and again until the roughness that is desired is obtained.

2.3 Remote Control's Effectiveness for a Machine of Surface Grinding

It has been observed that automation helps increase effectiveness. Studies conducted on remotely controlled machine have shown that these processes are way more time efficient and provide much more dimensional accuracy. Surface Grinding can also be improved by using a remotely controlled mechanism following a path planned by the operator. To plan a path the operator uses a CAD-based software such as AutoLISP of AutoDesk Co. A semiautomated feature for remotely controlled surface grinding is added to the machine. This basically develops a Man-Machine Interface (MMI).

The MMI works in the following steps:

Firstly, a path that has to followed is designed on the CAD software. The machine uses this path as a guide. This path is used as an optimum position for the machine to either start or to stop. The machine can follow four approaches in terms of directions: a) one-way vertical direction b) two-way vertical direction c) one-way horizontal direction, and d) two-way horizontal direction. For the path designing a relative coordinate system is used rather than an absolute coordinate system. Since the relative coordinate system, when displayed on the computer screen of the machine is difficult for the operator to understand, it has to be converted into absolute coordinate system to make it user-friendly. The Relative Coordinate System can be changed into Absolute Coordinate System by two methods: a) coordinate transposition and b) angle rotation. Coordinate transposition is found by comparing the distance between basis points of both the coordinates. In Eq. 15, dX denotes the distance in horizontal plane and dY denotes the distance in vertical plane. The value of X and Y are obtained using the GPS. Similarly, the angle rotation is found by calculating the angle θ between the axis of both the coordinates. The angle is also estimated using the GPS. After finding the coordinate transposition and angle rotation, their values are fed in the following two equations to convert relative coordinate system to absolute coordinate system:

$$\begin{aligned} Xr &= (x-dX)\cos(\theta) - (y-dY)\sin(\theta) \\ Yr &= (y-dY)\sin(\theta) + (x-dX)\cos(\theta) \end{aligned} \tag{15}$$

During the operation, the actual position of the spindle of the machine is located using a GPS. The data of the GPS is compared with the data of the path planned on the CAD software. This helps us to verify whether the machine follows a controlled path or not. In case the spindle deviates from the planned path during grinding the remotely controlled machine brings it back to the planned path. Actually, the trajectory of the spindle of grinding machine is being displayed on the computer screen, where it is being compared with the actual path. In this way the operator can make certain decisions to make the machining process precise and keep the system controlled.

Once the grinding process is completed the spindle returns back to its starting position.

Even if the most accurate GPS is used there might still be some error left. This might affect our dimensional accuracy a bit, but still, it is negligible. This machining process accompanied by remote control and path planning from GPS data provides much more dimensional accuracy than a simple spindle surface grinding machine.

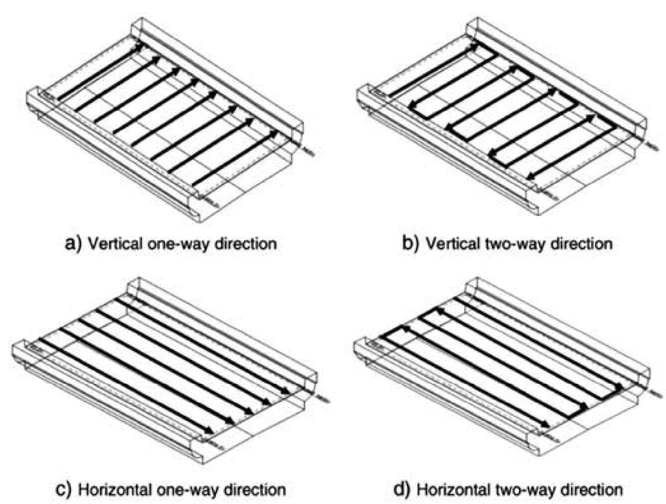

Figure 9: Movement direction in surface grinding [3].

2.4 Study of Control Organization's Study along with the Analysis of Performance for a Top Surface Grinding Machine

The system of control for a top surface grinding machine is now described, which is based on a Programmable Logic Controller (PLC). A brief description of PLC is show in Fig. 9.

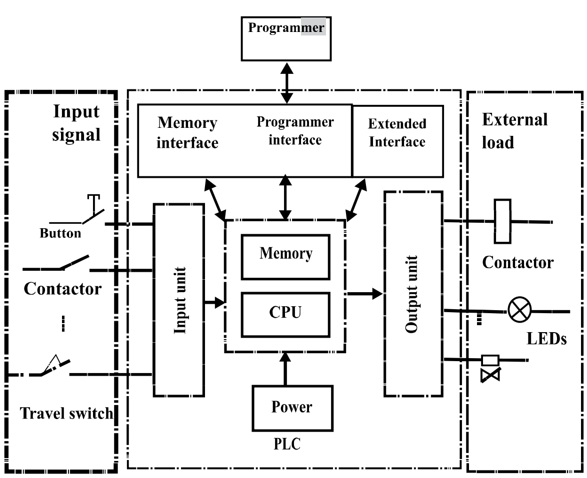

Figure 10: Working principle and composition Programmable Logic Controller (PLC) [7].

Grinding with precision is done on a machine equipped with units of mechanical and a controller. The machine comprises of chucks that is being mounted on an indexing table that firmly grips the workpiece under consideration while it is being operated. Two induction motors are used to rotate these chucks. Variable frequency drives control the speed of these motors.Initially, input pieces are added into the system through the belt of conveyor controlled by solenoid valves. The process of grinding is then divided into two phases: the pre-finishing phase and the finishing phase. Both of these phases use a similar grinding technique; the only difference is that the grinding wheels used at each station are different. The working principle of grinding consists of grinding wheels that are mounted on a spindle that is revolving, the motion of which is controlled by servo motors and sensors. The parts that operate the servo motor in the grinding system are known as servo drives. By continuously monitoring the feedback signal from the servo mechanism, a servo drive adjusts for variations from desired performance. This drive accepts a commanding signal from a system of control, then makes it amplified, after that sends servo motor an electric current to generate some sort of motion proportionate to the commanding signal. Some sensors of proximity are therefore installed; they provide input on the slide's movement. To grind, both the workpiece holding chuck and the grinding wheel spin. In-process gauging is performed during grinding at both stations, allowing the machine to impulsively adjust to the parts fluctuating length. Self-gauging of the workpiece is done, along with measured values are provided as a data for the system to control the machine for grinding purposes, provides for exact grinding of the workpiece. Human Machine Interface is connected to PLC and displays the information for operator there. The operator can make control decisions on the basis of this information. For this, the operator gives commands to PLC logic through HMI which in turn controls the system.

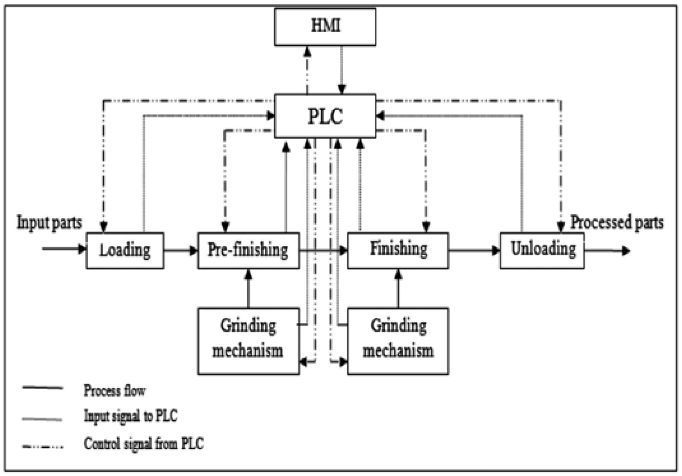

Figure 11: Schematic of control organization of surface grinding machine [7].

3. PROPOSED APPROACH

Control System of Compliance Feedback in Grinding for Part Parallelism

Certain models of grinding have indeed been developed for the sole purpose of planning trajectory in the vertical direction in order to improve vertical compliance. . Parallelism might improve if the track was followed in an open loop, according to numerical simulations. To increase the parallelism and provide a superior surface finish, a control system for feedback force and power are being used. However, there are some disadvantages in this open loop manner. The forces in grinding fluctuate greatly, the function of open-loop ramp becomes impossible to predict. Another drawback of the control system for open-loop function is that the path for each type of workpiece must be specified separately. This approach, however, can certainly be improved by setting the control system in a closed-loop manner. The method, discussed in this article, depends mostly on constantly changing the depth of cut of workpiece to accommodate for machine compliance fluctuations.

The force of vertical grinding force is measured with the help of a dynamometer. To track the projected deflection of the wheel, a tracking controller is utilized. The following section outlines the basic methodology, which is trailed by the evaluation of the compliance of machine, an investigation of the stability of system, an explanation of the facilities, and experimental procedure, along with the outcomes.

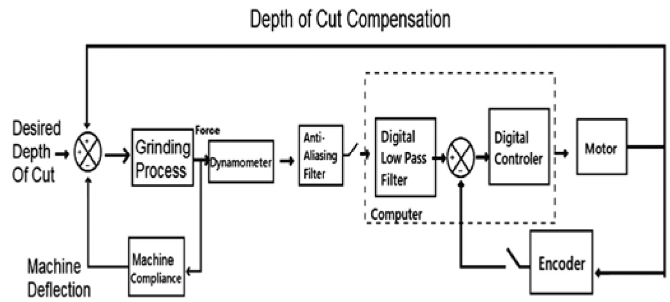

Figure 12: Controller's block diagram.

3.1 Compensation Methodology

It is known that grinding force and material removal rate have a direct relation. However, the material removal rate is inversely proportional to the cut's depth. So, force of grinding can reduce by decreasing the depth of cut. Another factor that effects the grinding force is the contact area among grinding wheel and workpiece, the more the area, the greater the force and vice versa. Since all the above-mentioned factors fluctuate during a machining process, the grinding force may vary owing to machine compliance. This lowers the finished workpiece's parallelism.

3.2 Compliance Modelling

Fig. 12 shows the block diagram of a controller which comprises of table of machine and the both compliances i.e., that of grinding wheel and the spindle's compliance. Here two models have been used to model compliance. The initial method involved bringing down a stationary grinding wheel over the workpiece and carrying out measurement of force produced using dynamometer. Fig. 13 shows the graph of the resulting connection as a dotted line. Here a compliance value of 7.1 x 10^{-5}mm N^{-1} was given in the form of a line equation as x = cmF.

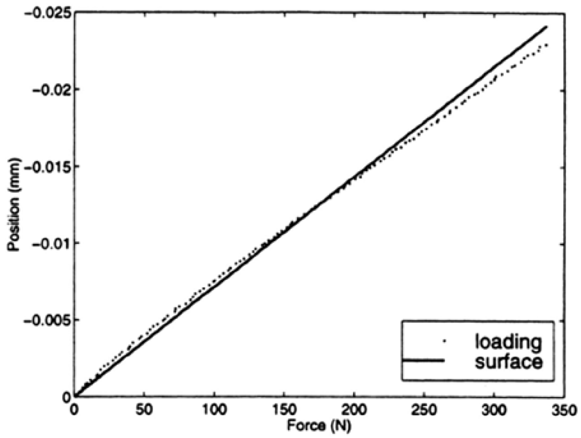

Figure 13: Measured compliance [1].

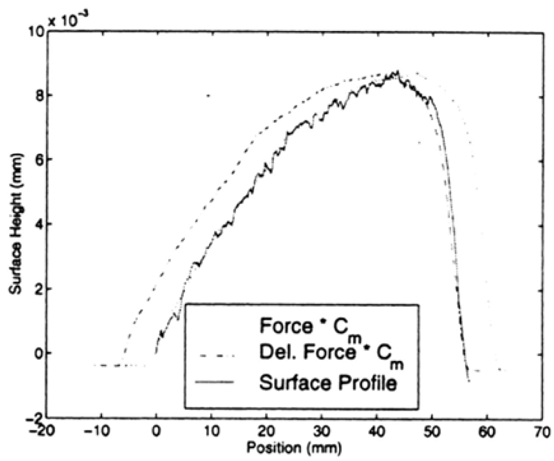

Figure 14: Force profile relationship. 0.0254 mm (0.001 in) nominal depth of cut. 762 (30 in min-1) feed rate. 7.31 x 10^{-5} mm N^{-1} compliance. The workpiece was a 57.15 mm (2.25 in) diameter 1018 steel cylinder [1]..

One method of measuring the machine's compliance independently was to correlate the force measured with the surface profiled workpiece. For the experiment, only the front half of the grinding wheel was run over the workpiece. Fig. 14, that depicts the relationship between surface profile and grinding force, clearly illustrates the surface profile that is measured by an LVDT by a solid line. Both the inside and the outside force lines indicate the wheel's edges of the wheel at the time the force was measured. A delayed force is produced by the inside edge. Compliance of Machine has been used to scale the force. About 21 experiments for numerous rates of feed and cut's depth, the value of compliance was determined to be 7.17 x 10^{-5}mm N^{-1} using the method least squares minimization of the surface that was being observed and the force that was scaled due to compliance.

3.3 Analysis of Stability

When a control system loop is used, the steady system of grinding can become wobbly. Therefore, to make the system stable, we have to adjust the cut's depth. The feed in horizontal direction is mostly the primary feed. The force generated by this feed is

$$F = \frac{AV_f}{K_g'} d_c \qquad (16)$$

Here V_f, V, d_c, A, K'_g represent the rate of feed,velocity of the grinding machine's wheel relative to workpiece under observation, depth of cut, contact's area among the workpiece and grinding wheel of the grinding machine, and constant of proportionality respectively. The feed owing to raising the depth of cut is the other direction of feed. This feed direction produces a force of

$$F = \frac{A}{K_g V} \dot{d}_c \qquad (17)$$

Here, $\dot{d}_c$ and K_g represent the rate at which the feeding of wheel into the workpiece is done and the proportionality constant, respectively. Now the transfer function is given by

$$\frac{F(s)}{d_c(s)} = \frac{A}{K_g V} s + \frac{AV_f}{K_g' V} = K_c(Rs + 1) \qquad (18)$$

$$where\ R = \frac{A}{K_g V}\ and\ K_c = \frac{AV_f}{K_g' V} \qquad (19)$$

Grinding stiffness is what the term Kc stands for. A second-order dynamic function with effective mass m, effective stiffness k, and the effective damping co-efficient b is now employed for stability analysis. In Fig. 15, K_f represents the positive feedback gain and T is the first-order filter with constant time. The depth of cut and force in this model can stated in the form a relationship as transfer function as:

$$G(s) = \frac{K_c K_f (Rs+1)(Ts+1)(ms^2+bs+k)}{a_0 s^3 + a_1 s^2 + a_2 s + a_3} \qquad (20)$$

$$\text{where} \quad a_0 = K_f T_m - K_c R_m$$
$$a_1 = K_f(m + bT) + K_c(R(K_f T - b) - m)$$
$$a_2 = K_f(b + kT) + K_c(R(K_f - k) + K_f T - b)$$
$$a_3 = kK_f + K_c(K_f - k)$$

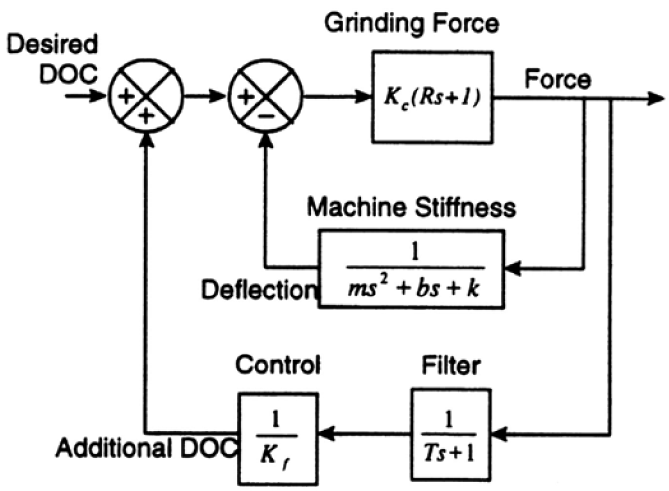

Figure 15: Model for stability analysis of grinding system [1].

Table 1: Parameters calculated through experiments

k	2.1 x 10^4 N m^{-1}
b	0.78 Ns m^{-1}
m	1.2 x 10^{-4} Kg
K_c	1.5 x 10^4 N mm^{-1}
T	0.044 s

For the control scheme to work and to get a positive value for a3, Kf is set approximately k. Also, for stability requirements we require positive a0. This causes Eq. (19) to become as follows:

$$\frac{A}{K_g V} < kT \qquad (21)$$

Another stability requirement for depends on the size of R. In this requirement there is a condition that $a1$ must always be positive.

Assuming k>>m and k>>b.

The limit on K_c as R approaches zero is determined by

$$\frac{K_c}{K_f} < 1 + \frac{bT}{m} \qquad (22)$$

Another requirement for stability is have a positive $a2$ as well as a positive $a_1a_2 - a_0a_3$ term. This leads to equation where

$K_f = k$.

$$\frac{K_c}{K_f} < \frac{bT}{2m}\left(1 + \sqrt{\left(1 + \frac{4m}{bT}\right)}\right) \qquad (23)$$

Various parameters in Table 1 were found experimentally.

3.4 Experimental Procedure

To verify the controller's capacity, twenty-one experiments were conducted with two distinct workpiece materials at varying feed rates and depths of cut. One of the workpieces was a 1018 steel cylinder with a diameter of 57.15 mm (2.25 in) while the other was a 4015 steel cylinder with a diameter of 49.0 mm (1.93 in). A vertical spindle surface grinding Computer Numerical Control machine was used for testing purposes.

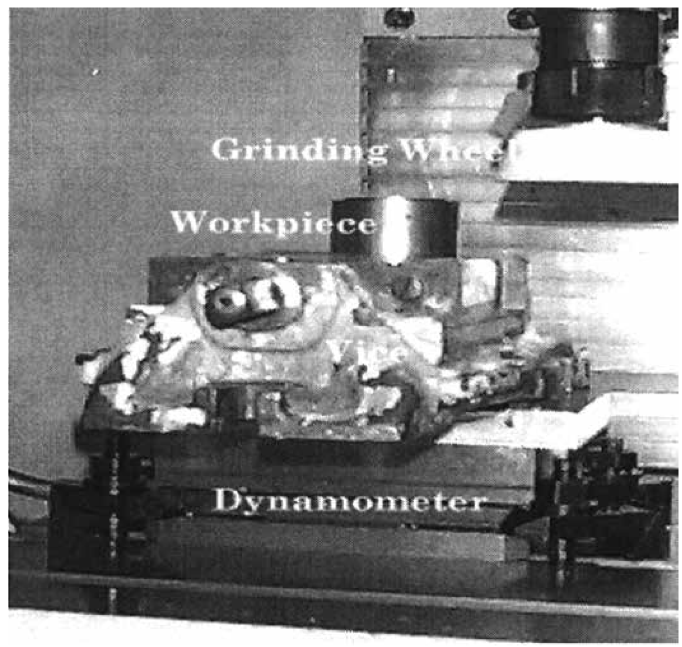

Figure 16: Setup configuration of grinding [1].

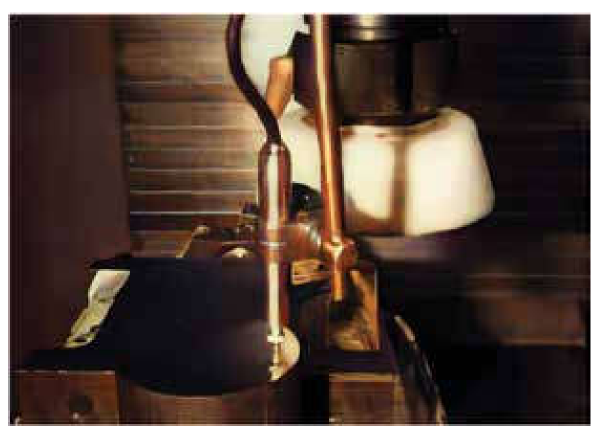

Figure 17: LVDT measuring surface profile of ground workpiece [1].

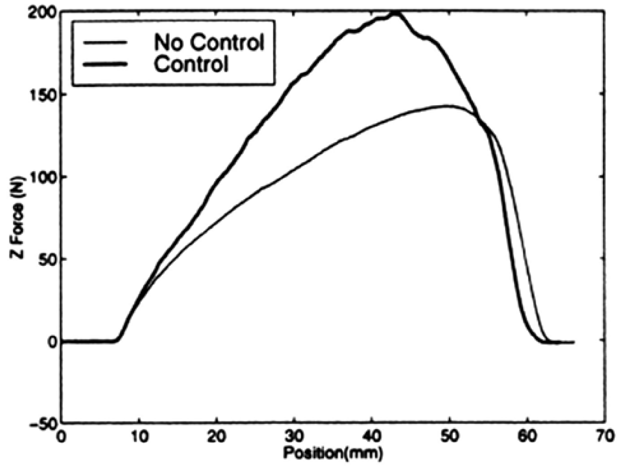

Figure 18: Comparison of measured force with respect to position with and without control. For second workpiece, depth of cut was 1016 mm min^{-1} (40 in min^{-1}), 0.0254 mm (0.001 in), spindle speed was 3000 r.p.m. [1].

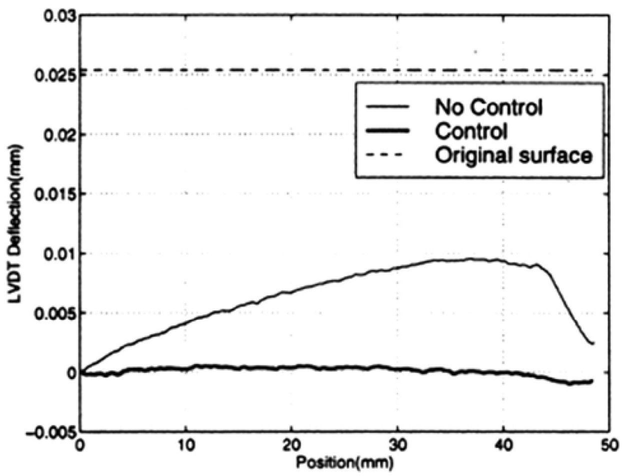

Figure 19: Improvement in surface profile with respect to LVDT Deflection and Position. For second workpiece, depth of cut was 1016 mm min^{-1} (40 in min^{-1}), 0.0254 mm (0.001 in), spindle speed was 3000 r.p.m. [1].

Tool path for closed-loop control system at a set feedrate is provided by commercial CNC machine tool controllers. This specified path, however, can just be selected off the path and will show no reaction to fluctuating cutting situations or the input sensor receives while machining. As a result, the circuitry of controller (Bridgeport Troq-Cut 22) utilized in the research was upgraded for the machine tool to be controlled by an external PC controller. For each and every axis of the grinding machine, a switch for multipole rotary was added. This switch can convert the output from the matching motor's encoders from being sent into the controller circuitry to being fed through an outside port of the grinding machine. The switch operated a relay, which switched the motor input from the controller circuitry's amplifier to an additional changing amplified breadth of pulsation. The input of amplifier's signal came from the similar outer connection. An external computer with a controller card may control the machine axis by axis using this port. Many other sensors can be read with the machine built in this way, for the sole purpose of monitoring process and improve the control system by giving extra information. For example, using the dynamometer to measure the force and using the force to derive the trajectory. The controller may also be utilized to synchronize position, force, and LVDT readings.

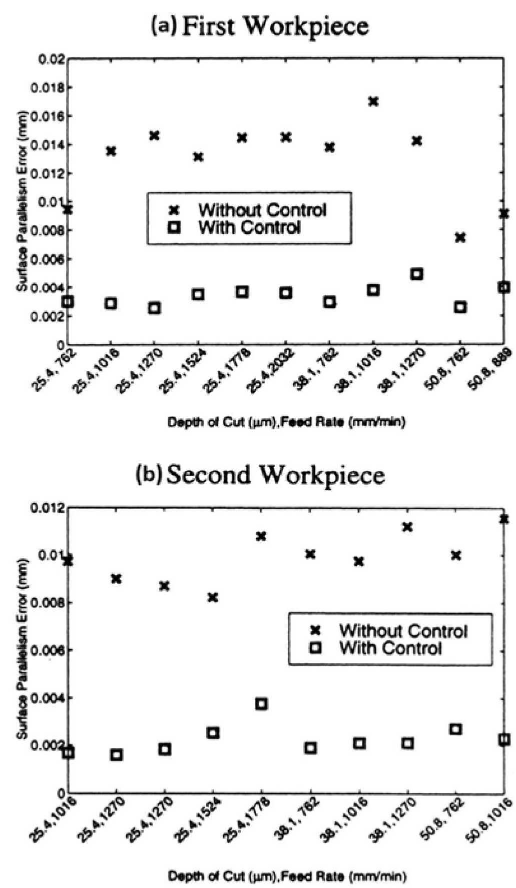

Figure 20: (a)Parallelism's comparison of first workpiece with and without control with respect to depth of cut and feed rate

(b)Parallelism's comparison of first workpiece with and without control with respect to depth of cut and feed rate [1].

Fig. 18 depicts force measured under control and without any control. The peak grinding force increases as the depth of cut increases, as expected.

Fig. 19 depicts an example of workpiece parallelism enhancement under the influence of control. As the grinding wheel exits the workpiece, the control system becomes more effective. Before this point the grinding wheel exits the workpiece, control system becomes greatly effective. This is due in part to the shifting cutting dynamics that occur when only the rear of the wheel removes material rather than the entire cup rim. The phase delay in the force measurement filter, which occurs when the wheel leaves the component and the force quickly changes, is another element to consider. Fig. 20 (a) and (b) depicts the resulting surface parallelism at various cut depths and feed rates. As the rate of feed and rate of material removal enhanced, so did parallelism enhance. In general, a surface having less error in parallelism error were obtained for the controlled workpiece, and with minimum accumulation on grinding wheel during the process of grinding.

First workpiece when controlled, the improvement in parallelism in terms of average was 72.5 % and for controlled second workpiece was 77.3 %. Surface Parallelism's improvement for first workpiece was greatly affected the material removal rate. Both had an inverse relation. Second workpiece's improvement falls as both feed rate of feed and the cut's depth rise. Similarly, when rate of material removal increases, the overall increase decreases.

4. METHODOLOGY

Grinding machine's functional capabilities, control systems, and peripheral process monitoring equipment have all improved during the last 20 years. Process enhancement technologies such as touch detection, wheel balancing, and in-process gauging may be incorporated into higher-end grinding machines based on customer requirements. The achievable single pass tolerances in vertical spindle surface grinding are frequently restricted by machine compliance and also the grinding wheel. The approach presented here involves precisely altering the depth of cut during grinding to maximize dimensional precision. It also resulted in a significant improvement in the quality of surface grinding.

A technique for controlling surface parallelism during the grinding process is offered by altering the depth of cut. Grinding wheel and machine compliance usually restrict single-pass tolerances in vertical spindle surface grinding. The proposed approach entails precisely changing the depth of cut during grinding to improve dimensional precision without the need for additional spark out passes. The correction is made in this situation based on the expected deflection from the simulated compliance as well as the observed vertical force.

Surface grinding's goal is to remove material quickly while maintaining the ideal workpiece size and form. The efficiency of surface grinding is mostly determined by the depth of cut (DOC). In surface grinding, the amount of grinding force is critical. A large depth of cut will result in a strong grinding force. Grinding chatter, burns, and exploding grinding wheels are all possible outcomes of unvaried grinding force. The variation of normal grinding force is seen in a surface grinding operation due to the unevenness of the component surface or of the grinder wheel. Also, increased depth of cut control may increase grinding force. Only a lesser average Force can be applied to the part surface to avoid scorching the work piece or injuring the grinder. If the grinding force is controlled to a constant value, the system will be able to achieve stability. The construction of the models and design of the controllers in this thesis is based on several key principles and results from control theories. For instance, transfer function, root locus, and so on. A transfer function is a mathematical depiction of the relationship between an LTI (linear time-invariant) system's input and output.

The Laplace transform is a valuable mathematical tool that helps solve and evaluate linear differential equation models with less effort. The root locus is the path traced out in the s-plane by the roots of the characteristic equation as a system parameter (usually a gain) is modified.

A method for enhancing surface parallelism in vertical spindle cup grinding is described in this paper. The strategy focuses on actively changing the depth of cut to compensate for the system's fast deflection. A dynamometer is positioned between the workpiece and the machining table to measure the vertical grinding force. Based on an off-line system compliance model, this force component is utilised to anticipate system deflection. The deflection is then tracked in real time using a tracking controller. When compared to when no control is employed, the approach provides a surface with reduced parallelism error. As a result of the feedback force control, the finished product has better consistency and tolerances.

The system's block diagram is provided by

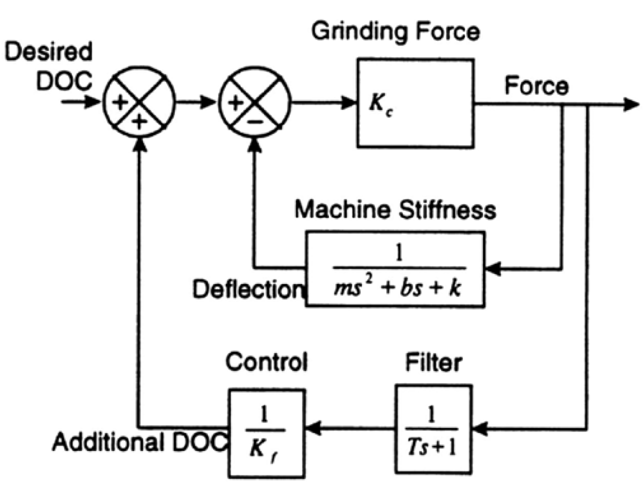

Figure 21: Block diagram of grinding system

The transfer function which was derived in the approach Compliance Feedback Control for Part Parallelism in Grinding is given by

$$G(s) = \frac{K_c}{1\frac{K_c}{ms^2+bs+K} - \frac{K_c}{K_f}\left(\frac{1}{Ts+1}\right)}$$

$$G(s) = \frac{K_f K_c(ms^2+bs+k)(Ts+1)}{K_f(ms^2+bs+k)(Ts+1) + K_f K_c(Ts+1) - K_c(ms^2+bs+k)} \quad (24)$$

$$G(s) = \frac{K_f K_c(ms^2+bs+k)(Ts+1)}{K_f(mTs^3+(bT+m)s^2+(kT+b)s+k) + K_f K_c(Ts+1) - K_c(ms^2+bs+k)}$$

Here K_c represents grinding stiffness, m represents effective mass, b represents effective damping coefficient, k refers to effective stiffness, T refers to time constant and K_f represents positive feedback gain.

From experiments, the measured values of the unknown parameters are

$K_c = 1.5x10^4$ N/mm
$K_f = 1410$
$m = 1.2x10^{-4}$ kg
$b = 0.78$ Ns/m
$k = 2.1x10^4$ N/m
T = 0 004 s

Substituting the values of parameters in Eq. (24), our transfer function becomes,

$$G(s) = \frac{10152s^3+68526000s^2+1793097000000s+444150000000000}{0.007448s^3+46.7604s^2+222839.8s+2250000} \quad (25)$$

The block diagram is then reduced, using Eq. (25), as follows

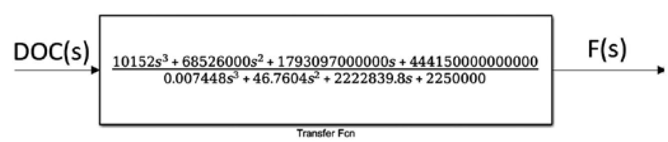

Figure 22: Reduced block diagram

This transfer function is converted into state space using MATLAB. Converting from state space to transfer function is straight forward since the transfer function form is unique. It's more harder to convert from transfer function to state space, owing to the wide number of state space forms that may be used to represent a system. The following is the code that was used for this:

Code 1: Transfer function

```
clc

clear all

close all

s=tf('s')

G=((10152*(s^3))+(68526000*(s^2))+(1793097000000*s)+444150000000000)/((0.007448*(s^3))+(46.7604*(s^2))+(2222839.8*s)+2250000)

Gss=ss (G) % this command is used to convert transfer function to state space.
```

The result obtained is as follows:

```
s =

s

Continuous-time transfer function.

G =

 10152 s^3 + 6.853e07 s^2 + 1.793e12 s + 4.442e14

 -----------------------------------------------

 0.007448 s^3 + 46.76 s^2 + 2.223e06 s + 2.25e06

Continuous-time transfer function.

Gss =

A =

          x1         x2         x3

 x1      -6278  -1.822e+04       -144

 x2  1.638e+04          0          0

 x3          0        128          0

B =

          u1

 x1  2.621e+05

 x2          0

 x3          0

C =

          x1         x2         x3

 y1       2453  -3.866e+04  1.077e+05

D =

          u1

 y1  1.363e+06

Continuous-time state-space model.
```

5. IMPLEMENTATION

The suggested grinding force controller is designed in MATLAB and verified in Simulink in this thesis. The following is a basic description of MATLAB and Simulink. MATLAB is a computer language used in scientific computing. It provides an intuitive interface that combines computation, visualisation, and programming with problems and solutions written in standard mathematical notation. Simulink is a MATLAB-integrated software tool for modelling, simulating, and analyzing dynamic systems. It provides a graphical environment in which dynamic systems can be designed, simulated, implemented, and tested.

Now the control system is tested with different types of inputs and is verified.

5.1 Step Input

The block diagram of step input is given by

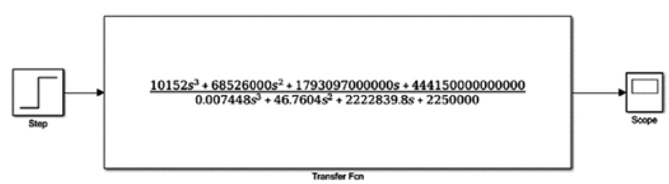

Figure 23: Block diagram of step Input

The graph of step input is given by

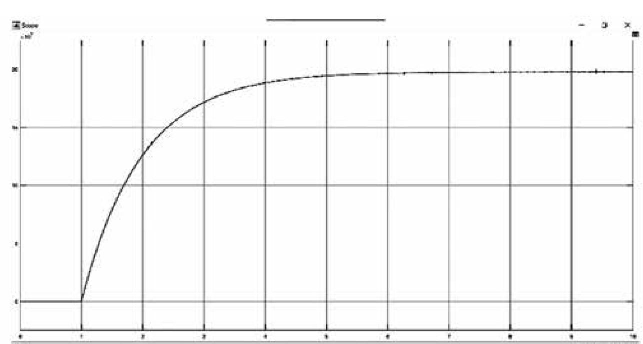

Figure 24: Graph of step input

From the graph, it is clearly observed that the system is quite stable. There are no overshoots in the system. The system gives a very good response to the step input. The graph shows that the system achieves stability after 6s. The system stays stable once the stability is achieved. This is indeed a good system.

5.2 Ramp Input

The block diagram of ramp input is given by

Figure 25: Block diagram of ramp

The graph of ramp input is given as

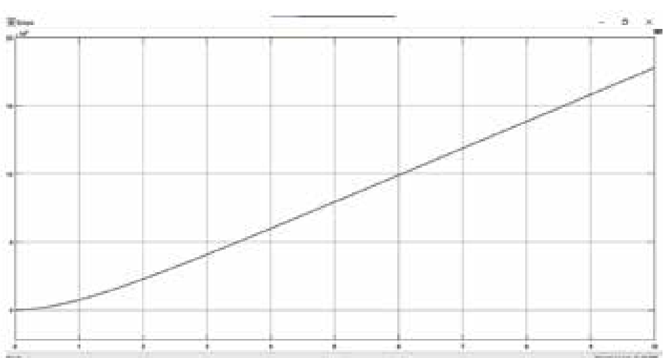

Figure 26: Graph of ramp

The ramp function is a one-dimensional unary real function with a ramp-like graph. The name "ramp" can also refer to various functions that are created by scaling and shifting, and the unit ramp function is the one discussed in this article (slope 1, starting at 0). The ramp function is also known as the positive portion in mathematics. The control system in the case follows the ramp in a quite good manner. This verifies that the system is a good system.

5.3 Parabolic Input

The block diagram of parabolic input is given as

Figure 27: Block diagram of parabolic input

The graph of parabolic input is given by

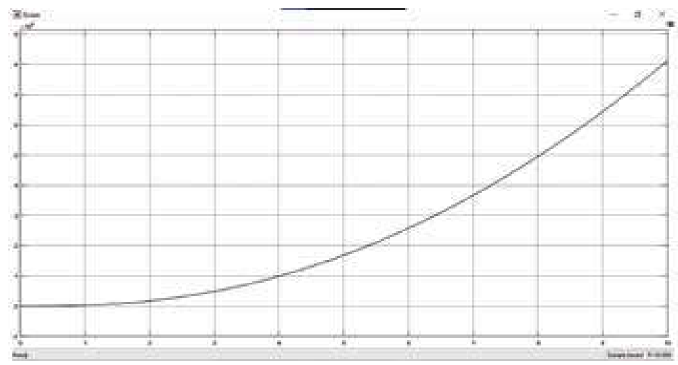

Figure 28: Graph of parabolic input

A signal is characterized as a parabolic signal or parabolic function when it gives a continuous acceleration differentiation from the real input signal. Unit acceleration signal is another name for it. At t = 0, the unit parabolic signal begins. Once again, the system follows a parabolic path without any disturbance in the system. Thus, it is evident that this is a good system.

5.4 Stability

The gain of the system is varied to check the stability of the system at various gains. This can also help the user to vary gains according to their needs. The transfer function of the system is given by

$$G(s) = \frac{10152s^3 + 68526000s^2 + 1793097000000s + 444150000000000}{5.28 \times 10^{-6} K_f s^3 + [0.003444K_f - 1.8]s^2 + [1584.78K_f - 11700]s + [22500K_f - 3.15 \times 10^6]}$$

Here K_f is the gain. Now to check the range of gain, K_f Routh Table is used.

The system's characteristic equation is provided by

$$5.28 \times 10^{-6} K_f s^3 + [0.003444K_f - 1.8]s^2 + [1584.78K_f - 11700]s + [22500K_f - 3.15 \times 10^6]$$

Now the Routh Table is given as

Table 2. Routh Table

s^3	$5.28 \times 10^{-6} K_f$	$1584.78 K_f - 11700$
s^2	$0.003444 K_f - 1.8$	$22500 K_f - 3.15 \times 10^6$
s	$5.28 \times 10^{-6}[22500 K_f - 3.15 \times 10^6] - [1584.78 K_f - 11700][0.003444 K_f - 1.8]$	
1	$22500 K_f - 3.15 \times 10^6$	

It is necessary to do the following in order to get positive numbers in the first column:

$5.28\times10^{-6}K_f>0 \Rightarrow K_f>0$
$0.03444K_f-1.8 >0 \Rightarrow K_f>52.26K_f$
$22500K_f- 31.5\times106 >0 \Rightarrow K_f>1400$
$[1584.78K_f -11700][0.03444K_f -1.8]- 5.28\times10^{-6} [22500K_f - 31.5\times10^6]> 0$
or
$54.52K_f^2 - 402.48K_f- 2852.6K_f+ 21060 >0.1188K_f^2-166.32K_f$
$54.4K_f^2- 3088.76 K_f+ 21060 >0$
or

$K_f^2- 56.8K_f+ 387.1>0$

or
$(K_f- 7.92)(K_f- 48.88)>0$
So either $K_f<7.92$ and $K_f<48.88 \Rightarrow K_f<7.92$
or $>7.92\, f\, K$ and $>48.88 \Rightarrow >7.92$

The fourth row stipulates the most dominant condition.

We now conclude requiring $K_f>1400$.

5.5 Steady State Errors

As time goes to infinity, the steady-state error is the difference between the desired and actual value of a system output in the limit (i.e. when the response of the control system has reached steady-state). In this situation, the steady state errors are as follows:

$$\lim_{s\to0} G(s) = \frac{4.4415\times10^{14}}{2250000} = 197.4\times10^6$$

$$e_{step(\infty)} = \frac{1}{1+\lim_{s\to0} G(s)} = \frac{1}{1+197.4\times10^6} = 5.066\times10^{-9}$$

$$e_{ramp(\infty)} = \frac{1}{\lim_{s\to0} sG(s)} = \frac{1}{0} = \infty$$

$$e_{parabola(\infty)} = \frac{1}{\lim_{s\to0} s^2\, G(s)} = \frac{1}{0} = \infty$$

Hence, from the above calculations, it is evident that the error in step input is negligible and that the errors in ramp and parabola are infinity.

5.6 Root Locus

By varying system gain K from zero to infinity, the Root locus is the location of the roots of the characteristic equation.

The root locus of the system is calculated using MATLAB and the graph of the root locus obtained is as follows:

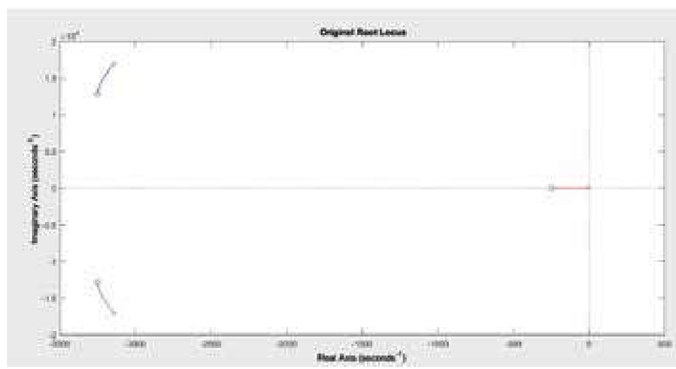

Figure 29: Root locus of system

The MATLAB code of root locus is given by:

Code 2: Matlab code for root locus

```
clc
clear all
close all
s=tf('s')
G=((10152*(s^3))+(68526000*(s^2))+(1793097000000*s)+444150000000000)/((0.007448*(s^3))+(46.7604*(s^2))+(2222839.8*s)+2250000)
rlocus(G)
```

The graph shows that all of the system's poles and zeros are located on the system's left half plane, indicating that the system is stable. One of the poles is quite close to but not at the origin, indicating that the system is extremely stable. The system becomes unstable if the poles are in the right half plane.

The controller's resilience to disturbances and parameter modifications should be determined since it remained stable across a wide range of settings.

6. RESULTS

The transfer function of the system which is shown in Eq. (25) was in third order.

$$G(s)=\frac{10152s^3+68526000s^2+1793097000000s+444150000000000}{0.007448s^3+46.7604s^2+222839.8s+2250000}$$

To solve the system easily and to find its characteristics, it is reduced to second order system using MATLAB using balred command.

$$G(s)=\frac{2.665 \times 10^6 s^2+6.264 \times 10^{10} s+1.555 \times 10^{13}}{s^2+7.781 \times 10^4 s+7.7876 \times 10^4} \quad (26)$$

Upon resolving the system to second order, its rise time, settling time, natural frequency and damping frequency can easily be found.

For this system Settling time Comes out to be 0.00876s

Rise time comes out to be 0.0158s

$\omega_n = 3.943 \times 10^6$
$\zeta = 7.99428 \times 10^3$

Since the value of ζ is greater than 1, our system is overdamped.

The MATLAB code used for finding the above parameters is as follows:

Code 3: For finding parameters

```
clc
clear all
close all
num=[10152 68526000 1793097000000 444150000000000];
den=[0.007448 46.7604 2222839.8 2250000];
G=tf(num,den);
T=balred(G,2)
 G1=feedback(T,1);
  [numt,dent]=tfdata(G1,'v');
omegan=sqrt(dent(3))
  zeta=dent(2)/(2*omegan)
```

The system's response without any controller was as follows

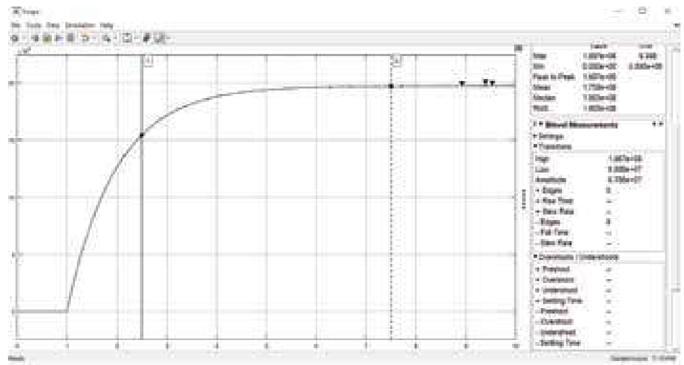

Figure 30: System's response without any controller

A controller is a component in a control system that attempts to close the gap between a system's actual value (i.e. the process variable) and its desired value (i.e. the setpoint). All modern control systems need controllers, which are an integral aspect of control engineering.

Controllers may be used for a number of different purposes, such as:

- By minimizing steady-state error, controllers increase steady-state accuracy.
- Improvement of steady-state accuracy leads to improvement of stability.
- Furthermore, controllers assist in the eradication of unneeded offsets in the system.
- Controllers can be used to regulate the system's maximum overrun.
- Utilizing controllers can serve to minimize noise signals in a system.
- An overdamped system's delayed response can be sped up by using controls.

When the plant's performance isn't matching the system's standards, a closed loop control system, rather than a new plant, might be beneficial. The controller was derived from the difference between the actual and necessary outputs. This controller, in turn, causes the plant to take the appropriate corrective steps, bringing the actual output closer to the desired one.

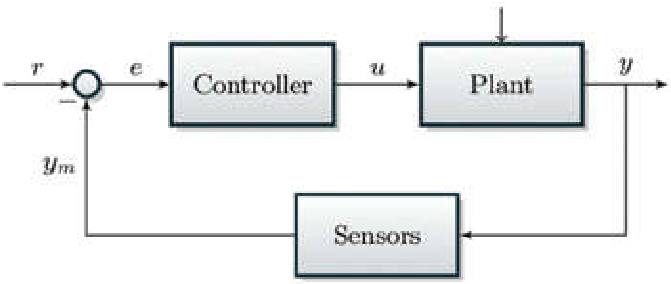

Figure 31: Schematic of a controller

Errors are of two types

- Transient Error
- Steady State Error

The most basic way is to create an actuating signal u proportionate to the error, with the actuating signal's magnitude growing as the error grows. This allows the real output to correspond to the required output. This is the proportional controller. This controller is beneficial when the error is below a specified threshold. If the error exceeds a certain threshold, a proportional controller is insufficient to handle it.

The plant's reaction to the input when it is applied is delayed as a result of the reluctance. When the gain of the proportional controller is increased to reduce the delay, the controller overshoots, resulting in oscillations at the output. A transient error is what it's called. It's now time to think about how much the rate of change in error has changed as a result of the control operations.

Overshoot and oscillatory behavior can be regulated if the rate of change of error at the point of crossing the final value is utilized to manage the plant's output. The derivative controller is based on this concept. This controller should be used with caution when the signal contains noise, which is very typical. The noise is amplified by the derivative controller, which causes the plant to become unstable.

However, because to some intrinsic constraints, the plant may never reach the designated point. The steady state mistake is the result of this. For detecting this steady state error, the integral of the error will yield a superior response. The steady state error can then be reduced using the error integral. An Integral controller is based on the concept of employing a constant error across time. This controller improves the plant's performance in noisy environments.

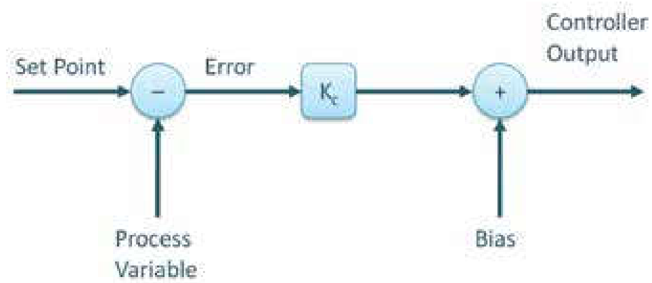

Figure 32: Schematic of P controller

To reduce the rise time and increase response speed, a proportional controller is used. The phase response of the plant is not influenced by this controller.

Here K_p=25

The graph of the system is plotted using Simulink on MATLAB

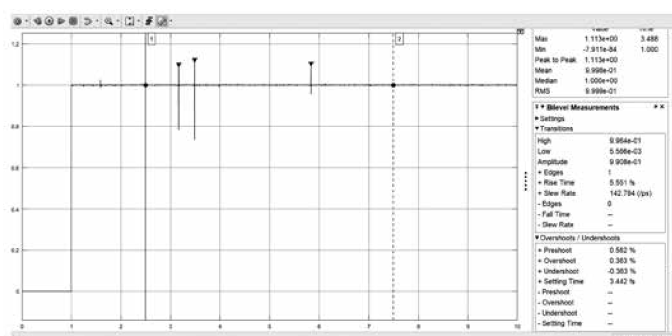

Figure 33: System's response with P controller

6.1 PI Controller

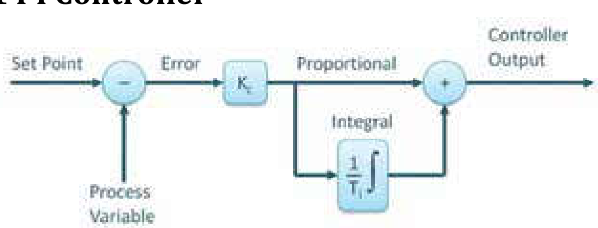

Figure 34. Schematic of PI Controller

This comes in handy when proportional control is needed to speed up settling and integral control is needed to decrease error that is constant throughout time. PIC (Proportional Integral Control) is a controller type (PI controller). The rising time and steady state errors of a system can be reduced with the use of a PI controller. When you need to modify magnitude and phase at the same time, this tool will come in helpful.

Here $K_p = 25$

$K_i = 20$

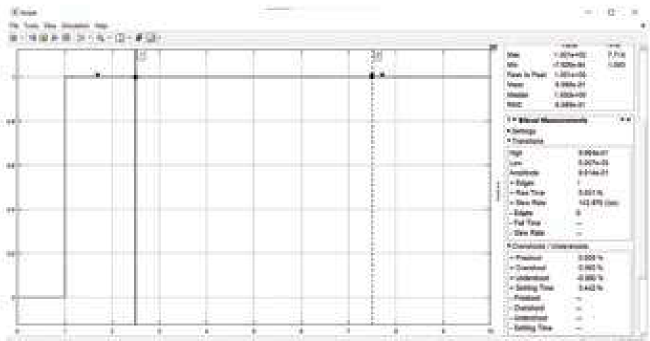

Figure 35: System's response with PI Controller

6.2 PID Controller

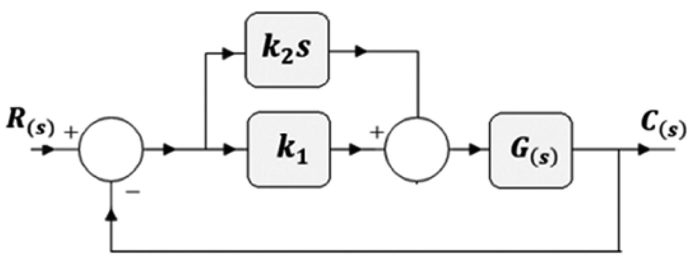

Figure 36: Schematic of PD controller

In practice, no one controller is capable of completing the job. Many controllers must work together to meet the criteria. When we need to speed up the transient time, we utilize proportional control, and for overshoot and oscillation difficulties, we use derivative control. As a result, a proportional-derivative controller is required (PD Controller). The signals must be noiseless; otherwise, the derivative actions would exacerbate the noise, causing the plant to lose stability. The PD controller reduces output transients such rising time, overshoot, and oscillations. This is handy when altering magnitude and wishing to add phase led to the output.

Here $K_p = 25$

$K_d = 0.00001$

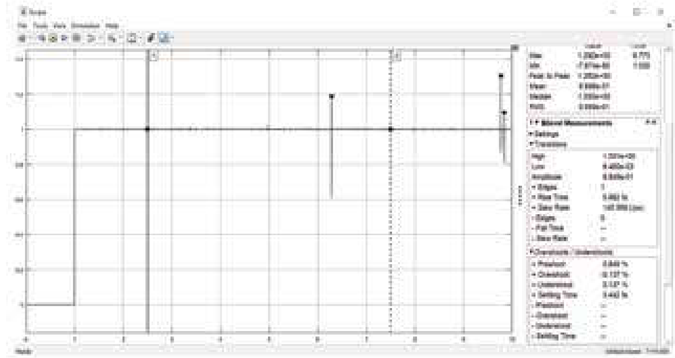

Figure 37: System's response with PD controller

6.3 PID Controller

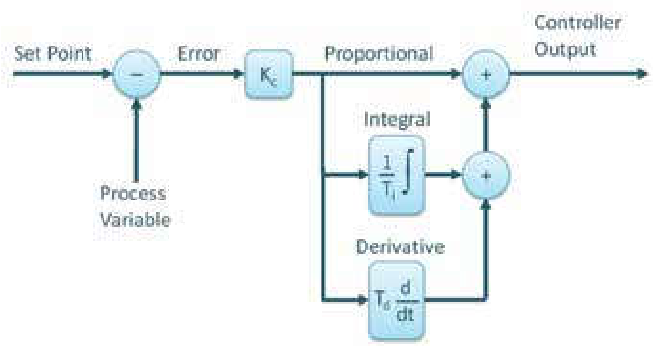

Figure 38: Schematic of PID controller

Solving all of the difficulties listed above with a single solution is a more broad example. In this case, all three controllers are utilized in conjunction with appropriately determined gains. By changing these gains, any combination of P, I, D controllers may be obtained, resulting in a more robust controller. A PID controller is a type of controller that may be applied to a wide range of applications. By modifying the gains of the three control actions, any controller may be created. This wide type of controller may produce a magnitude change as well as a lead or lag in phase in the output.

Here $K_p = 25$

$K_i = 20$

$K_d = 0.00001$

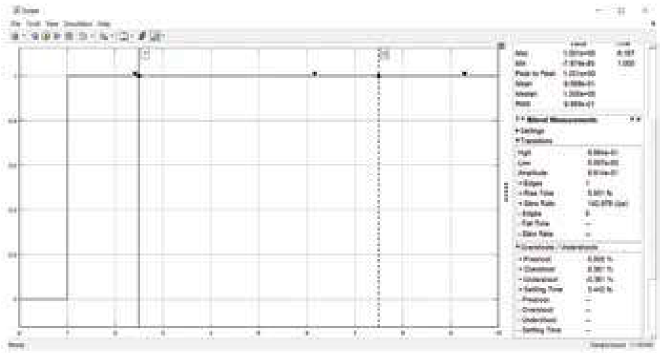

Figure 39: System's response with PID controller

7. CONCLUSION

Grinding classification is a common complicated system, and regulating the grinding and classification system for automated concentrators has proven to be a challenging and time-consuming operation. Grinding classification is a critical component of the mineral processing industry's production processes and product size management, and its effects have a direct impact on the quality and efficiency of flotation concentrate product recovery operations. As a result, using advanced intelligent control technology to ensure its product size qualified premise of improving grinding and classification production efficiency, lowering production costs for enterprises to improve beneficiation economic efficiency and market competitiveness in the grinding and classification process has significant practical significance.Control of unattended production processes and machinery, as well as automatic counselling to inexperienced employees, are becoming increasingly important in today's manufacturing environment. This research looks at the design and performance of an autonomous process controller for traverse grinding, with an emphasis on decreasing chatter vibration-induced waviness on the machined surface. This was accomplished by employing a range of model-based wheel regeneration chatter monitoring and mitigation tactics, which has been highlighted as the most challenging problem to handle in big industrial roll grinding machines during roughing and semi-finishing processes. Low labor skills, a labor scarcity, and poor quality can all have a negative impact on operational performance when it comes to surface grinding. A method for enhancing surface parallelism in vertical spindle cup grinding is described in this paper. The strategy focuses on actively changing the depth of cut to compensate for the system's fast deflection. A dynamometer is positioned between the workpiece and the machining table to measure the vertical grinding force in this method. Based on an off-line system compliance model, this force component is utilised to anticipate system deflection. The deflection is then tracked in real time using a tracking controller. The technique produces a surface with less parallelism error as compared to when no control is used. To demonstrate the compensating technique, grinding tests were carried out. The results demonstrate that the approach is effective at a variety of feed rates and cut depths. The most noticeable parallelism gain is around five times, with effectiveness dropping somewhat when the federate and cut depth were increased. Parallelism was improved in all circumstances, with a minimum of a 50% improvement. The findings of this study open up the possibility of improving machine tolerance or throughput by minimizing the number of sparkout passes required.

8. RECOMMENDATIONS

A surface grinder's principal function is to remove material from a flat surface in order to finish the workpiece to the desired size and finish with a fine surface finish. They're also used to sharpen cutting tools, grind small flanges, as well as large cylinder blocks, machine bases, and a variety of other products. Any engineering industry would be incomplete without a Surface Grinding Machine. Your machine has gotten more accurate and productive since CNC Controls were introduced. Surface Grinding Machines are necessary in every business, whether it is the car, consumer goods, or machine tool manufacturing.

To support the exploitation of the solution industry, the controller can be upgraded by adding more diagnostic functions to control the mechanical confusion that may interfere with control functions. In addition, speeding operations should include not only the stability of the cutting process, but also other technical limitations and competency features such as roughness and appearance, as well as the production and cost of the entire system. The controller can also be customized to work with various grinding machines due to the flexibility of the design.

REFERENCES

[1] Hekman, K. A., & Liang, S. Y. (1999). Compliance Feedback Control for Part Parellelism in Grinding. The International Journal of Advanced Manufacturing Technology, 15(1), 64–69. doi:10.1007/s001700050040 J. Clerk Maxwell, A Treatise on Electricity and Magnetism, 3rd ed., vol. 2. Oxford: Clarendon, 1892, pp.68–73.

[2] A. K. Srivastava and M. A. Elbestawi, "Control strategy formultipass robotic grinding", International Journal of Robotics andAutomation, 10 (3), pp 114–119, 1995

[3] Moon, S., Yang, B., Kim, J., & Seo, J. (2010). Effectiveness of remote control for a concrete surface grinding machine. Automation in Construction, 19(6), 734–741. doi:10.1016/j.autcon.2010.03.001

[4] Ning, D., Jingsong, D., Chao, L., & Shuna, J. (2019). An Intelligent Control System for Grinding. 2019 IEEE 3rd Information Technology, Networking, Electronic and Automation Control Conference (ITNEC). doi:10.1109/itnec.2019.8729268

[5] Manoj Kumar,Jyoti Raman,Priya Priya , "Particle Swarm Optimization: Intelligent Neural Network System (PSOINNS) Based Multi-Objective Optimization of Surface Grinding Operations" , International journal of materials forming and machining processes;2334-4563; vol.2; no.1; p.54-87, 2015

[6] X. Shuqin, "Application of PLC in Computer Numerical Control Machine", International Conference on Industrial Electronics and Applications (IEA), 2015.

[7] Shital A. Dhatrak, Vitthal J. Gond, "Study of Control Organization of a Top Surface Grinding Machine with its Performance Analysis", International Research Journal of Engineering and Technology, 2016.

[8] Li, Y., & Zhou, S. (2018). Sensorless balance method for the spindle system of computer numerical control gear grinding machine. Measurement and Control, 002029401880271. doi:10.1177/0020294018802715

[9] Shih YP and Chen SD. A flank correction methodology for a five-axis CNC gear profile grinding machine. Mech Mach Theory 2012; 47: 31–45.

[10] Yue C, Ren X, Yang Y, et al. Unbalance identification of speed-variant rotary machinery without phase angle measurement. Shock Vib 2015; 2015: 11.

[11] LUO Fuyuan,YOUYoupeng,YIN Juan. Research on the Algorithm of NURBS Curve Bidirectional Optimization Interpolation with S-type Acceleration and Deceleration Control [J].Chienes Journal of Mechanical Engineering,2012,48(5):147-156

[12] S.Bououdena, M.Chadlib,H.R.Karimic.An ant colony optimizationbasedfuzzy predictive control approach for nonlinearprocesses[J].Information Sciences,2015.4(299):143-158

[13] Mukherjee I, Routroy S. "Comparing the performance of neuralnetworks developed by using Levenberg–Marquardt and Quasi-Newton with the gradient descent algorithm for modelling a multipleresponse grinding process". Expert Systems with Applications, vol.39,No.3,pp.2397-2407, 2012.

[14] Jiang, X., Guo, M., & Li, B. (2017). Active control of high-frequency tool-workpiece vibration in micro-grinding. The International Journal of Advanced Manufacturing Technology, 94(1-4), 1429–1439. doi:10.1007/s00170-017-1015-5

[15] Chen F, Liu G (2017) Active damping of machine tool vibrations and cutting force measurement with a magnetic actuator. Int J Adv Manuf Technol 89:691–700

[16] Guo M, Li B, Yang J, Liang SY (2016) Influence of dynamic force on vibration of micro-machine tool spindle. Proceedings of the International Conference on Advanced Materials, Structures and Mechanical Engineering, 217–222

[17] Parenti, P., Leonesio, M., & Bianchi, G. (2016). Model-based adaptive process control for surface finish improvement in traversegrinding.Mechatronics,36,97-111. doi:10.1016/j.mechatronics.2016.04.001

[18] Michael, E. H. C., & Andre, B. D. (2017). Development of Control System for Vibratory Grinding Process. Procedia Engineering, 174, 1093–1099. doi:10.1016/j.proeng.2017.01.262

[19] Li, Y., & Zhou, S. (2018). Sensorless balance method for the spindle system of computer numerical control gear grinding machine. Measurement and Control, 002029401880271. doi:10.1177/0020294018802715

[20] Yixu, S., Hongjun, Y., & Hongbo, L. (2013). Intelligent Control for a Robot Belt Grinding System. IEEE Transactions on Control Systems Technology, 21(3), 716–724. doi:10.1109/tcst.2012.2191587

[21] WANG, H., LIU, J., DUAN, H., PAN, Y., ZHANG, Z., & YUE, S. (2019). Prediction Method of Rotation Speed of Workpiece on Camshaft Grinding Machine based on T-S Fuzzy Control. 2019 IEEE 3rd Advanced Information Management, Communicates, Electronic and Automation Control Conference (IMCEC). doi:10.1109/imcec46724.2019.8983936